

**Document Version**

Final published version

**Licence**

CC BY-NC-ND

**Citation (APA)**

Schaper, L., Tankova, T., da Silva, L. S., & Knobloch, M. (2022). Effects of state-of-the-art residual stress models on the member and local stability behaviour. *Steel Construction*, 15(4), 244-254. <https://doi.org/10.1002/stco.202200027>

**Important note**

To cite this publication, please use the final published version (if applicable).  
Please check the document version above.

**Copyright**

In case the licence states "Dutch Copyright Act (Article 25fa)", this publication was made available Green Open Access via the TU Delft Institutional Repository pursuant to Dutch Copyright Act (Article 25fa, the Taverne amendment). This provision does not affect copyright ownership.  
Unless copyright is transferred by contract or statute, it remains with the copyright holder.

**Sharing and reuse**

Other than for strictly personal use, it is not permitted to download, forward or distribute the text or part of it, without the consent of the author(s) and/or copyright holder(s), unless the work is under an open content license such as Creative Commons.

**Takedown policy**

Please contact us and provide details if you believe this document breaches copyrights.  
We will remove access to the work immediately and investigate your claim.

# Effects of state-of-the-art residual stress models on the member and local stability behaviour

Residual stresses have considerable effect on both the local and the member stability behaviour of steel structures. Previous studies have shown that the structural stability behaviour depends on both the distribution and the amplitude of the residual stresses. The residual stress distribution is affected by the cross-section geometry, the steel grade and the manufacturing process, e.g. flame cutting and the welding procedure. A realistic consideration of residual stresses is necessary for an efficient and safe design of steel structures.

This article presents an experimental and numerical study on the influence of residual stresses on the stability behaviour of structural members, i.e. steel columns and beams considering a variety of cross-sectional slenderness, i.e. plastic, compact and slender cross-sections are taken into account. A novel residual stress model for welded I-shaped sections was developed and evaluated using test data. This model takes into account the main influencing parameters, i.e. the cross-sections geometry, the steel grade as well as manufacturing process with thermal cuts or non-thermal cuts of the steel plates. The novel residual stress model is then used to investigate the stability behaviour in terms of a numerical simulation study. The result of the study allows to propose an improvement of the buckling curve selection for welded high strength steel columns and beams.

**Keywords** residual stresses; stability behaviour; local buckling; welded girders; flame cut

## 1 Introduction

Steel structures are characterized by the slenderness of both the cross-section and the member. The range of rolled sections and the possibility to produce various welded cross-sections allow an economical design adapted to the respective load situation. The manufacturing processes related to the application of local heat input, e.g. flame cutting, plasma cutting and welding, normally cause residual stresses that may have a significant effect on the structural stability behaviour.

Idealized residual stress models are used for the direct application in advanced numerical simulations, i.e. the model according to ECCS publication No. 33 [1] was commonly used in recent years. However, this model was

calibrated on steel members made of steel grades S235 and S355 in the early 1980s. Nowadays, state-of-the-art manufacturing processes and high strength steels are increasingly used; hence, adaption of residual stress models is necessary. Therefore, the model according to ECCS has been adopted in the upcoming prEN 1993-1-14:2021 [2] with an adaption for the use of a wide range of steel grades with a conservative approach. However, a comprehensive validation of this model, especially for high-strength welded steel structures, as well as a study on the influence on the stability behaviour are still missing.

The distribution of residual stresses has been investigated in recent studies, which address different issues. For example, effects of the cross-section shape and dimensions [3, 4], the steel grade [5, 6] and fabrication process [7] on the residual stress distribution have been studied. Up-to-date data collection of residual stress measurements including evaluation of the magnitude of the residual stresses related to the steel grade is part of [8]. These investigations show that the distributions can distinctly differ from the approaches according to ECCS and prEN 1993-1-14:2021 commonly used in design and research.

Systematic investigations on the influences of residual stress approaches on the structural stability behaviour are scarce. Käsmeier [9] analysed the influence of residual stress approaches according to [1] for hot-rolled and welded steel sections on the member stability behaviour, in particular the evolution of yield zones and, subsequently, the internal forces. The effect of a welded residual stress approach on the local-buckling behaviour for the example of three I-sections with slender webs is presented in [10]. Granath [11] focused on the development of plastic strains for slender plate girders, taking into account a residual stress approach for welded sections according to BSK94 [12].

A novel model for residual stresses of welded I-shaped doubly and mono-symmetric sections was jointly developed by the University of Coimbra and the Ruhr-Universität Bochum [13]. It considers both the cross-section geometry and the fabrication process with or without thermal cutting of the plates. A comparative study with both own and independent residual stress measurements available in the literature confirms that the model is suitable for steel members of steel grade S235 up to S890. This model is now applied to analyse comprehensively the local and structural member stability behaviour of welded steel sections.

This is an open access article under the terms of the Creative Commons Attribution-NonCommercial-NoDerivs License, which permits use and distribution in any medium, provided the original work is properly cited, the use is non-commercial and no modifications or adaptations are made.



ording to the novel model with and without thermal cuts and prEN1993-1-14 [2]. Geometric imperfections were applied with the shape of the relevant eigenmode for the considered member stability case with a maximum amplitude of  $L/1000$ . For the simulation of the cross-sectional and local buckling behaviour, additional nodes at the end of the weld legs have been used and connected with constraints (rigid beams). This represents on the one hand the stiffness of the joint between web and flange plates, and on the other hand reduces the length of the outstanding flange to consider the weld geometry for the local buckling behaviour. The relevant eigenmode for local buckling was determined on short girders with a ratio of girder length to flange width of approximately 4 and applied with a maximum amplitude of the twist with  $1/50$  radians of the outstanding flange.

The numerical model was validated within the framework of two German national research projects carried out at University of Stuttgart and Ruhr-Universität Bochum [15, 17]. Within these projects, structural member tests were performed at the University of Stuttgart for beams with major axis bending and beams with interactions of compression force, bending moments and torsion.

## 4 Influence of residual stresses on the load bearing behaviour

### 4.1 General

This Section summarizes the results of the parametric study. Firstly, the investigations on major and minor axis flexural buckling as well as lateral torsional buckling with influences of different shapes and distributions of residual stresses due to thermal and non-thermal cuts are provided (Section 4.2). Secondly, the effects of different cross-section geometries on the residual stress distributions and, accordingly, on the member stability behaviour are presented (Sections 4.3 to 4.5). Here, the decisive parameter of the section width as well as the weld thickness are varied. Subsequently, results are presented for members with different steel grades and thus different ratios of residual stresses to material strength (Section 4.6). Finally, effects of the residual stress approach on the local buckling behaviour and, in particular, the structural stability resistance of cross-sections with slender flange plates are shown (Section 4.7).

### 4.2 Effect of thermal and non-thermal cuts

Steel plates can be manufactured by non-thermal cutting processes, i.e. shearing, or by thermal cutting processes, such as plasma or flame cutting from the origin plate sheet. Thermal cutting methods cause tensile stresses at the position of the introduced heat and, for equilibrium reasons, compressive residual stresses in the remaining plate. When steel plates are assembled by welding, the residual stresses resulting from the welding process are

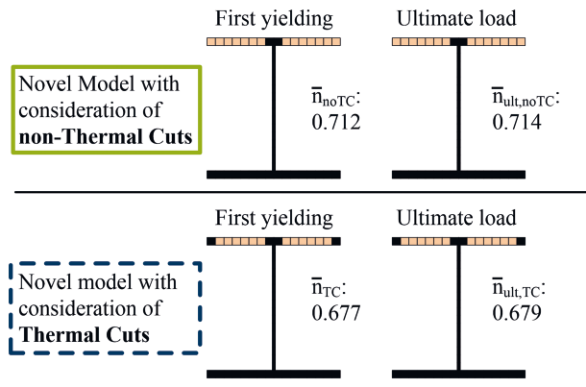
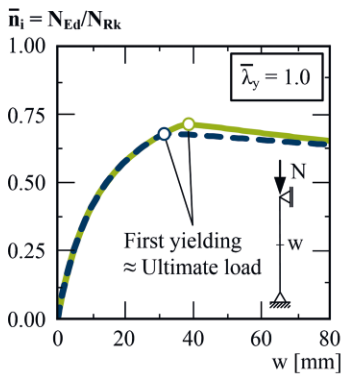
superimposed on the residual stresses of the cutting process. Thus, the residual stresses of thermal cut I-sections differ from the residual stresses from non-thermal cut I-sections.

The novel residual stress model for thermal cut plates, presented in Section 2, considers the manufacturing of the steel plates in two ways. These are (1) tensile residual stresses at the flange tips and (2) subsequently larger compressive residual stresses along the flanges compared to the residual stress approach with the consideration of non-thermal cuts. To illustrate the influence of these different residual stress approaches on the stability behaviour, numerical simulations were performed on a member with an exemplary cross-section considering major and minor axis flexural buckling as well as lateral torsional buckling in terms of a proof-of-concept study. The load-displacement behaviour and the development of the yield zones as a function of the non-dimensional load-factor are shown in Fig. 2.

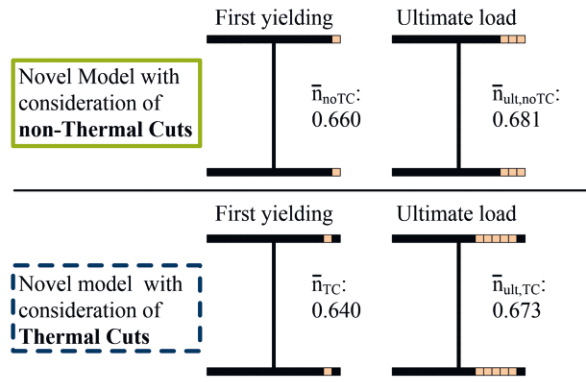
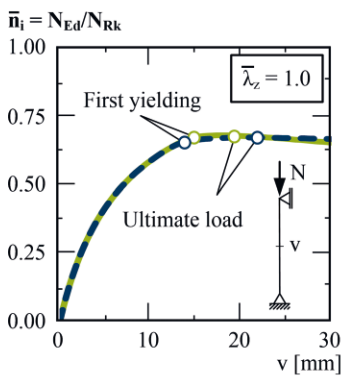
In case of major axis flexural buckling (Fig. 2, top), the mid-span deflection  $w$  increases with increasing load until the first yielding occurs at the flange because of the superimposition of compressive stresses resulting from axial compression force as well as bending moments according to second-order theory and the compressive residual stresses. When the non-thermal cuts are considered, the entire flange yields with the exception of the mid-flange in the area of the weld, while when the thermal cuts are taken into account, the flange tips remain in the elastic range and exhibit residual stiffness. However, after the initial yielding in both residual stress approaches, load increases are no longer possible due to the pronounced loss of stiffness, and stability failure occurs almost immediately. Since the compressive residual stresses at the flanges were smaller for the approach with non-thermal cuts, the first yielding and stability failure occur at higher load levels than for the approach with thermal cuts.

The out-of-plane displacement  $v$  in case of minor axis flexural buckling also increases until yielding (Fig. 2, middle). The location of the first yielding varies depending on the residual stress approach. When non-thermal cuts are considered, the first yielding occurs at both flange tips with compressive stresses resulting from second-order theory bending moments, while when thermal cuts are considered, the yield strength is firstly reached at the flange inner surface at the outer edge of the compressive residual stresses. Subsequently, however, small additional load-carrying capacities can be activated in both approaches until the ultimate load is reached. This is because of the progressive yielding in the flange towards the flange centre until stability failure. Nevertheless, similar ultimate load capacities are obtained for both residual stress approaches. When non-thermal cuts are considered, the lower compressive residual stresses overlap with the maximum stresses due to the bending moment at the flange tips, while when thermal cuts are considered, the higher compressive residual stresses overlap with the

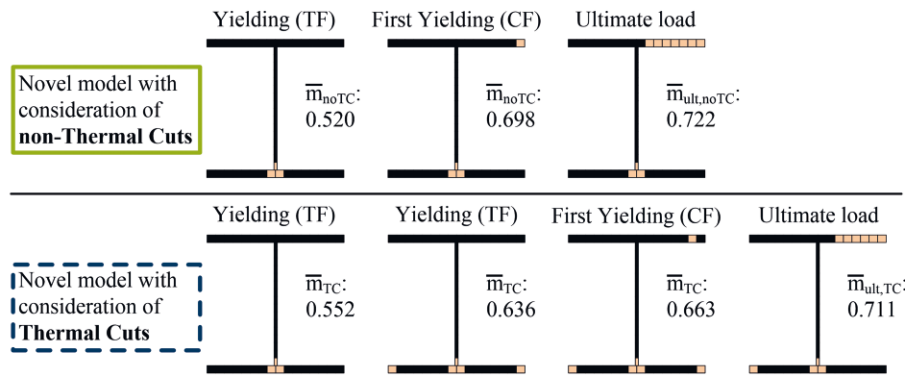
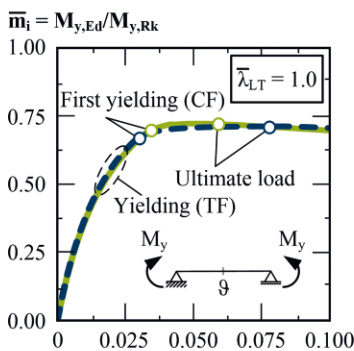
**Major axis flexural buckling**



**Minor axis flexural buckling**



**Lateral torsional buckling**



— Plastifications

Cross-section: flanges – 350 x 20 mm; web – 370 x 8 mm; double-fillet welds with a = 4 mm; S355

**Fig. 2** Development of yield zones depending of the stability case and residual stress approach

non-maximum stresses due to the bending moment at the inner position of the flange.

In case of lateral torsional buckling (Fig. 2, bottom), the load-displacement curves are like those of minor axis flexural buckling. However, the evolution of the yield zones in this case is different depending on the residual stress approach. The first yielding occurs at the centre of the tension flanges (TF) for both approaches due to the superposition of the tensile residual stresses at the weld and the tensile stresses caused by bending moment about the major axis. The differences in the load states at first yielding result from the residual stress applications in the numerical simulations. In addition, the flange tips of the tension flange (TF) reach the yield strength considering thermal cuts. However, the resulting reduction in stiffness is small and does not have a decisive effect on the load-

bearing behaviour. The stability failure is initiated with the first yielding at the compression flange (CF). The evolution of the yield zones at the compression flange is again comparable to minor axis flexural buckling. When non-thermal cuts are considered, yielding starts at the flange tips and progresses toward the flange centre, while for thermal cuts, the first yielding occurs at the inner flange and continues until stability failure. Here, the ultimate loads of the members are similar for both residual stress approaches.

The investigations on the stability behaviour have shown that the load-bearing behaviour differs depending on the residual stress approaches. Differences on the evolution of the yield zones result from tensile residual stresses or compressive residual stresses at the flange tips considering thermal or non-thermal cuts, while load capacities

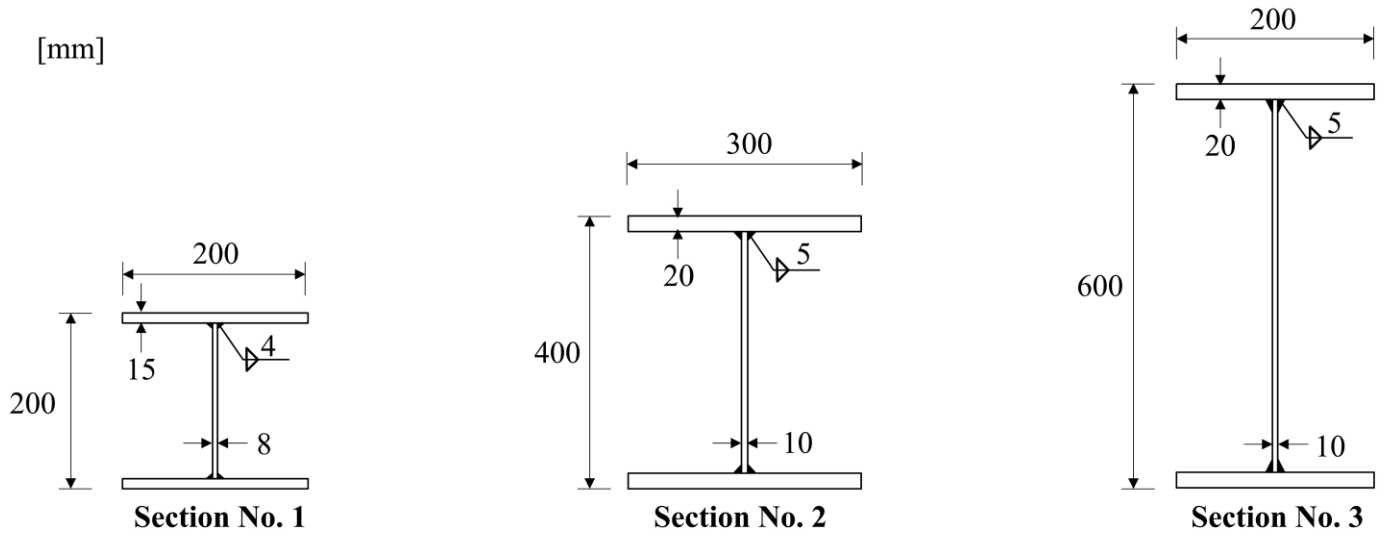


Fig. 3 Considered cross-sections for numerical simulations

can be affected by the different magnitude of the compressive residual stresses at the flanges. However, the consideration of thermal or non-thermal cuts has a marked effect on the load capacities in case of major axis flexural buckling and a minor effect in the cases of minor axis flexural buckling and lateral torsional buckling. The consideration of thermal cuts leads to lower member resistances. Since the influences of the residual stress approaches with or without thermal cuts are similar for minor axis flexural buckling and lateral torsional buckling, but differ for major axis flexural buckling, results for major axis flexural buckling and lateral torsional buckling are presented in the subsequent subsections in terms of a parametric study.

### 4.3 Influence of the cross-sectional slenderness

The cross-section geometry influences both the residual stress pattern according to the novel model and the stability behaviour. For the analysis of the influence of the cross-section geometry, three cross-sections were exemplarily considered and the results were evaluated within the framework of a comparative study. Here, section No. 1 is representative for stocky cross-sections, section No. 2 for cross-sections with an intermediate slenderness and section No. 3 for slender cross-sections (see Fig. 3).

Tab. 1 summarizes the magnitude of the residual stresses of the different sections of steel grade S355. Tensile re-

sidual stresses in the area of the weld are related to the steel grade and were therefore the same for all sections. If thermal cuts of the origin steel plates are considered, tensile residual stresses occur at the flange tips, which are related to the steel grade, too. Compressive residual stresses at the flanges depend on the cross-section geometry and the steel grade because of equilibrium conditions. This results in larger compressive residual stresses for narrow flange widths (section No. 1 and section No. 3) than for wider flanges (section No. 2) and higher compressive residual stresses at the flanges with larger weld and web thicknesses (section No. 1 compared to section No. 3). Furthermore, the fabrication of the steel plates has a significant effect on the residual stress distribution at the flanges with larger compressive residual stresses for thermal cut plates and smaller compressive residual stresses for non-thermal cut plates. The residual stress distribution at the web were simplified and determined without variations of the cross-section geometry and are therefore the same for all sections.

Fig. 4 illustrates numerically determined reduction factors in case of major axis flexural buckling (Fig. 4a) and lateral torsional buckling (Fig. 4b) compared to the buckling curves according to FprEN 1993-1-1:2022 [18] (paragraph 8.3.1.3 for flexural buckling and paragraph 8.3.2.3 (3) for lateral torsional buckling). The figure compares the results for the three sections with residual stress approaches according to the novel model with and without the consideration of thermal cuts. In case of major axis flexural buck-

Tab. 1 Residual stress magnitude according to the novel model

	$f_y \cdot \epsilon$ [MPa]	$0.5 \cdot f_y \cdot \epsilon$ [MPa]	Section No. 1 (S355)		Section No. 2 (S355)		Section No. 3 (S355)	
			$\sigma_{f,c}$ [MPa]	$\sigma_{w,c}$ [MPa]	$\sigma_{f,c}$ [MPa]	$\sigma_{w,c}$ [MPa]	$\sigma_{f,c}$ [MPa]	$\sigma_{w,c}$ [MPa]
Novel model <b>with</b> thermal cuts	288.8	144.4	-79.6	-72.2	-68.2	-72.2	-98.0	-72.2
Novel model <b>without</b> thermal cuts	288.8	-	-47.2	-72.2	-38.2	-72.2	-61.3	-72.2

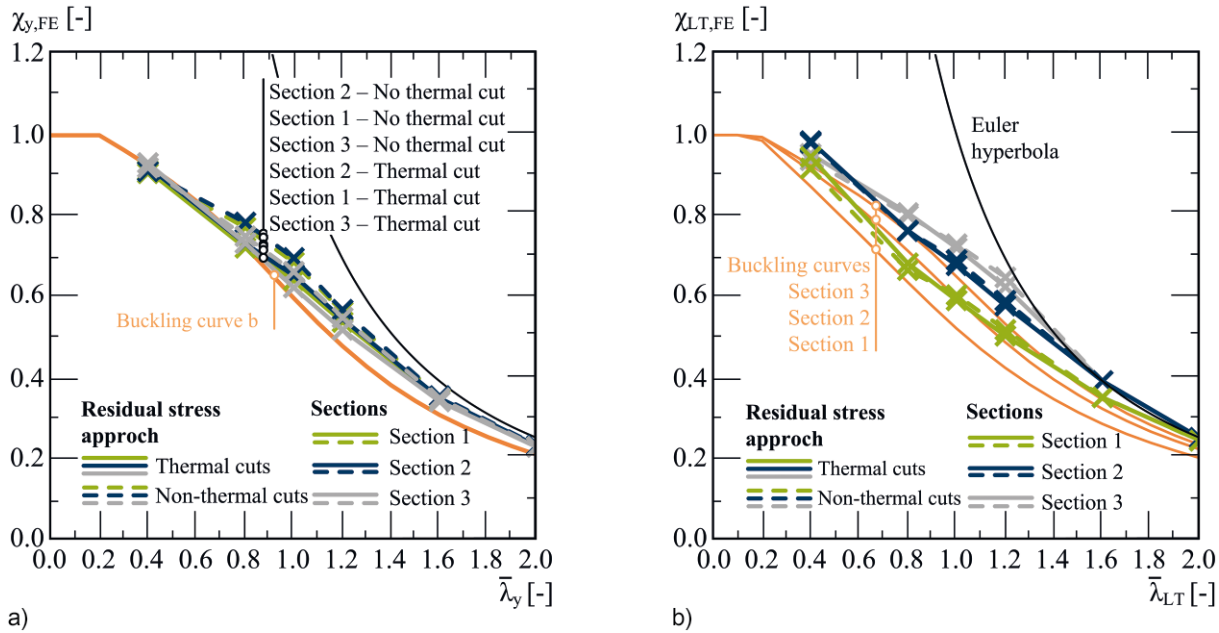


Fig. 4 Flexural buckling about the strong axis (a) and lateral torsional buckling (b) with different cross-sections and residual stress approaches

ling, higher reduction factors were achieved with consideration of non-thermal cuts compared to the consideration of thermal cuts. This effect occurs most strongly in the range of medium relative slendernesses ( $0.8 \leq \bar{\lambda}_y \leq 1.2$ ) with a relative deviation for the different residual stress approaches up to 7.1%. This is caused by the lower compressive residual stresses considering non-thermal cuts or larger compressive residual stresses at the flanges considering thermal cuts, respectively, and subsequent failure by reaching the yield strength in this area (see Section 4.2).

In case of lateral torsional buckling, a strong effect of the cross-sections geometry was observed but a minor effect of the residual stress approach with and without thermal cuts. The maximum relative deviation depending on the residual stress approach amounts to 3.7%, whereby the consideration of thermal cut plates tends to lead to smaller reduction factors. The relatively small deviation between the residual stress approaches for stability failure characterized by deformation about the weak axis (minor axis flexural buckling and lateral torsional buckling) is caused by the loss of stiffness at comparable load levels (see Section 4.2).

#### 4.4 Influence of the weld thickness

The size of the weld thickness is related to the width of the area affected by tensile residual stresses in the centre flange. The larger the area of tensile residual stresses in the flange, the larger the compressive residual stresses because of equilibrium conditions. The influence of the weld thickness on the change of compressive residual stresses at the flanges and thus the influence on the stability behaviour was analysed.

For section No. 3, numerical simulations with weld thickness between 2 mm and 5 mm (equal to half of the web

thickness) were performed. Fig. 5 shows the results for major axis flexural buckling (Fig. 5a) and lateral torsional buckling (Fig. 5b). The graphs show the numerically determined reduction factors on the left vertical axis and the compressive residual stresses on the right vertical axis as a function of the weld thickness, given on the horizontal axis. Blue lines indicate the behaviour based on the novel residual stress model considering thermal cuts and green lines are used for the novel residual stress model considering non-thermal cuts. Dashed lines represent the magnitude of the compressive residual stresses in the flanges that are decisive for the stability behaviour, while straight lines indicate the associated reduction factors.

The compressive residual stresses increase with increasing weld thickness. This results in compressive residual stresses from  $-61$  MPa for 2 mm weld thickness to  $-98$  MPa ( $= -0.28 \cdot f_y$ ) for 5 mm weld thickness considering thermal cuts or  $-32$  MPa ( $= -0.09 \cdot f_y$ ) for 2 mm weld thickness to  $-61$  MPa for 5 mm weld thickness considering non-thermal cuts.

In case of major axis flexural buckling the reduction factors for stocky members ( $\bar{\lambda}_y = 0.4$ ) and slender members ( $\bar{\lambda}_y = 1.6$ ) are constant regardless of weld thickness, with no significant difference between the residual stress approaches. This is due to the failure in the fully plastic or elastic range, respectively, where residual stresses have only minor effects. In the medium slenderness range ( $0.8 \leq \bar{\lambda}_y \leq 1.2$ ), the reduction factors decrease with increasing weld thickness and differ depending on the residual stress approach considered. Thereby, the reduction factors correlate with the magnitude of the compressive residual stresses related to the weld thickness or residual stress approach.

In case of lateral torsional buckling, similar effects can be expected as a function of relative slenderness. Neverthe-

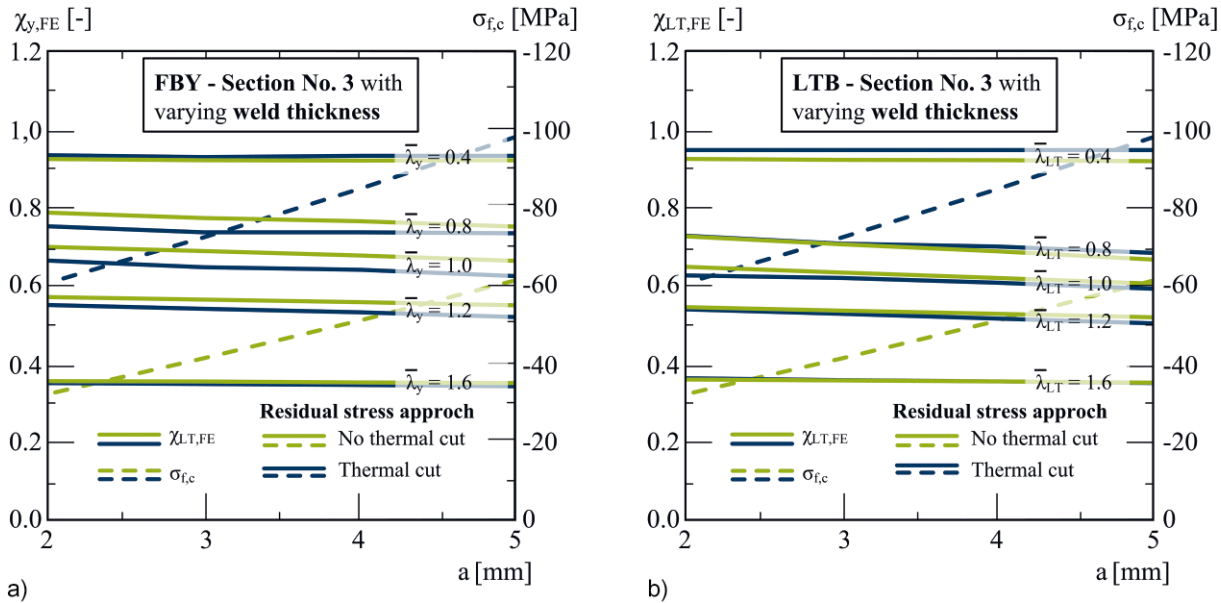


Fig. 5 Influence of the weld thickness on major axis flexural buckling (a) and lateral torsional buckling (b) considering different residual stress approaches

less, the reduction factors do not differ significantly depending on the residual stress approach in the range of medium slendernesses. This is due to the already mentioned different positions of the first yielding at the compression flange under similar load conditions (see Section 3.2).

Although the weld thickness has a considerable influence on the maximum compressive stresses, this results in only minor differences for the ultimate loads. This applies regardless of the residual stresses being influenced by thermal cutting or not.

#### 4.5 Influence of the flange width

The area of the flanges affected by compressive residual stresses is determined as the remaining area of the flange after taking into account the area affected by tensile residual stresses and is thus strongly dependent on the flange width. This results in smaller compressive residual stresses for wide sections and larger compressive residual stresses for narrow sections. To analyse the influence of this effect on the stability behaviour, the flange width of section No. 2 was varied from 150 mm ( $h/b = 2.67$ ) to 400 mm ( $h/b = 1.00$ ). As before, the compressive residual stresses of the flanges as well as the reduction factors were determined (Fig. 6). The determination of the slenderness as well as the reduction factors is based on plastic cross-section capacities for all cross-section classes in order to achieve a unified evaluation.

The magnitude of the compressive residual stresses decreases with increasing flange width, with the curves becoming flatter with larger width. The magnitudes differ from  $-112$  MPa ( $= -0.32 \cdot f_y$ ) at a width of 150 mm to  $-55$  MPa at a width of 400 mm considering thermal cuts, and from  $-72$  MPa at a width of 150 mm to  $-28$  MPa

( $= -0.08 \cdot f_y$ ) at a width of 400 mm considering non-thermal cuts, respectively.

The greatest effect of different flange widths and thus different compressive residual stresses occurs for medium relative slenderness ratios in the range of 0.8 to 1.2 for both major axis flexural buckling and lateral torsional buckling. Here, the reduction factors increase with increasing flange width. For major axis flexural buckling of members with medium slenderness ratios ( $0.8 \leq \bar{\lambda}_y \leq 1.2$ ), differences are present depending on the residual stress approach. The residual stress approach taking into account thermal cuts leads to smaller reduction factors compared to the approach with non-thermal cuts, caused by the higher compressive residual stresses at the flanges. The residual stress distribution does not lead to pronounced effects on the load-carrying capacity for lateral torsional buckling.

#### 4.6 Influence of the steel grade

The welding process can lead locally to residual stresses up to the yield strength [13]. These residual stresses drop sharply across the flange thickness, resulting in lower membrane stresses that are crucial for stability verifications. Nevertheless, the steel grade influences the magnitude of the membrane residual stresses, even if this is not proportional to the yield strength.

Tab. 2 compares the magnitudes of residual stresses as a function of the steel grade for section No. 3 considering the novel model with thermal cuts. Both compressive residual stresses and tensile residual stresses increase with increasing steel grade. Since the residual stresses are not proportional to the yield strength, but are defined by the material parameter  $\epsilon$ , a uniform factor of  $\sqrt{690/355} = 1.39$  is obtained between the respective quantities for the steel grades considered. Since residual stresses are less pro-

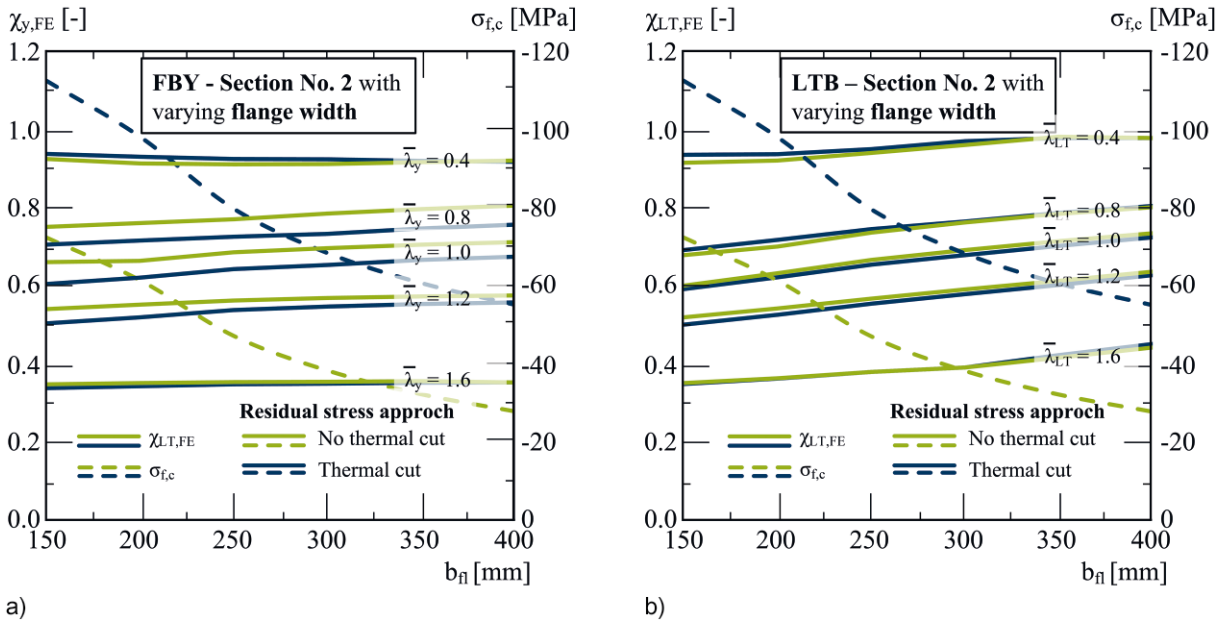


Fig. 6 Influence of the flange width on major axis flexural buckling (a) and lateral torsional buckling (b) considering different residual stress approaches

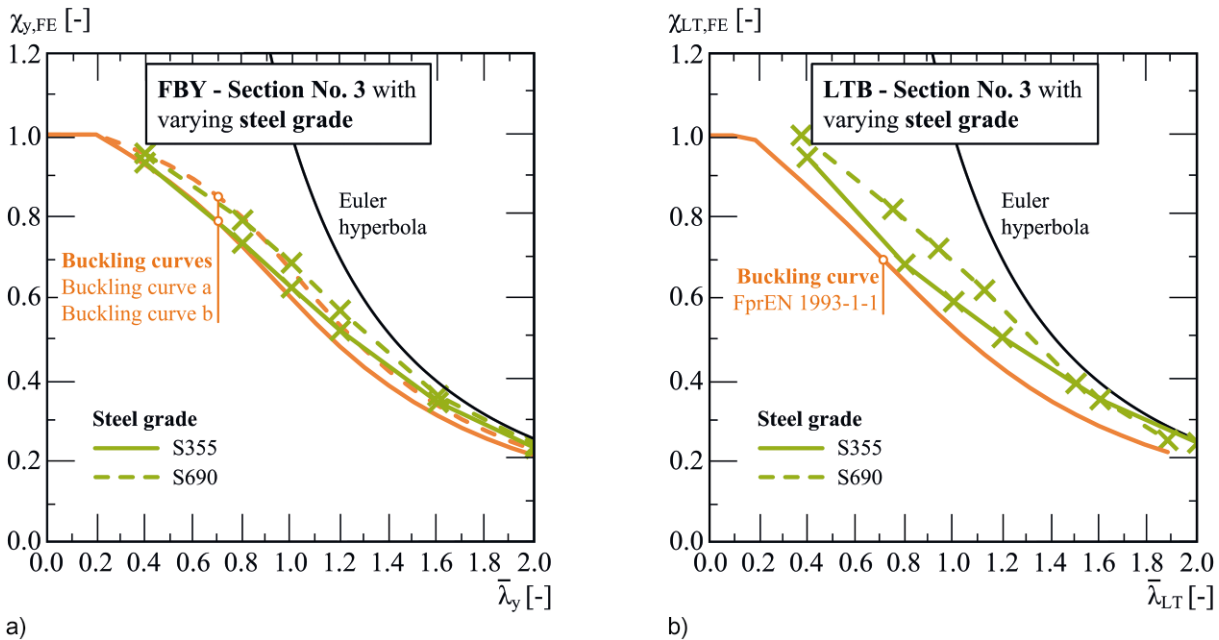


Fig. 7 Influence of the steel grade on major axis flexural buckling (a) and lateral torsional buckling (b) considering the novel model with thermal cuts

nounced for high strength steel, a higher ratio between ultimate load and cross-sectional capacity can be expected than for mild steel members.

Fig. 7 shows the reduction factors for major axis flexural buckling (Fig. 7a) and lateral torsional buckling (Fig. 7b) considering the novel residual stress model with thermal cuts. The reduction factors for section No. 3 made of steel grades S355 and S690 are compared with the buckling curves according to FprEN 1993-1-1:2022 [18]. For both flexural buckling and lateral torsional buckling stability phenomena, the reduction factors for S690 are larger. In the case of major axis flexural buckling, the section is assigned to buckling curve ‘b’ regardless of the steel grade. For high-strength steel, however, assignment to buckling curve ‘a’ is appropriate. The reduction factors for lateral

torsional buckling of the high-strength steel member are also approximated too conservatively, which seems to allow a more economical choice of imperfection coefficients and buckling curves.

#### 4.7 Effect on the cross-sectional capacity

Residual stresses influence the local buckling behaviour of slender cross-sections. While residual stresses have a minor effect on the rotational capacity and plastification of compact cross-sections, the behaviour of slender cross-sections, which buckle in the elastic range before reaching the cross-section capacity according to plastic theory, is decisively influenced. Therefore, in this study, the behaviour of welded I-sections made of mild steel S355 with

**Tab. 2** Residual stress magnitude according to the novel model

Steel grade	$f_y \cdot \epsilon$ [MPa]	$0.5 \cdot f_y \cdot \epsilon$ [MPa]	$\sigma_{f,c}$ [MPa]	$\sigma_{w,c}$ [MPa]
S355	288.8	144.4	-97.8	-72.2
S690	402.8	201.3	-136.6	-100.7

a height of 400 mm and a width of 300 mm (see Fig. 8) was investigated as an example. The web thickness of 6 mm was chosen to avoid local web buckling. The flange thickness was varied between 6 mm and 20 mm. This allowed to consider cross-sections, which are classified from class 2 to class 4.

The cross-sectional capacity related to the flange slenderness is also presented in Fig. 8. The numerically determined ultimate bending moment normalized by the plastic load capacity is shown on the ordinate and the slenderness of the flange plate is shown on the abscissa. Residual stress approaches according to the novel model with and without thermal cuts as well as the approach according to FprEN 1993-1-14:2021 [2], as illustrated in [13], are evaluated. The residual stress approach did not affect the load capacities of stocky cross-sections (class 1 and class 2) due to their ability of plastification. With increasing slenderness of the flange (class 3), the load capacities begin to differ for different residual stress approaches. This impact becomes more pronounced as the influence of local buckling increases (class 4). Here, the highest load capacities are reached considering the novel model with thermal cuts, slightly lower capacities considering the novel model without thermal cuts. Considering the residual stress approach according to prEN 1993-1-14:2021, the lowest load-capacities were determined. These load-capacities deviate up to 6% compared to the novel model for class 4-sections ( $12 < c_f/t_f \leq 20$ ).

The influences of residual stresses on the cross-sectional capacity are thoroughly analysed using an exemplary

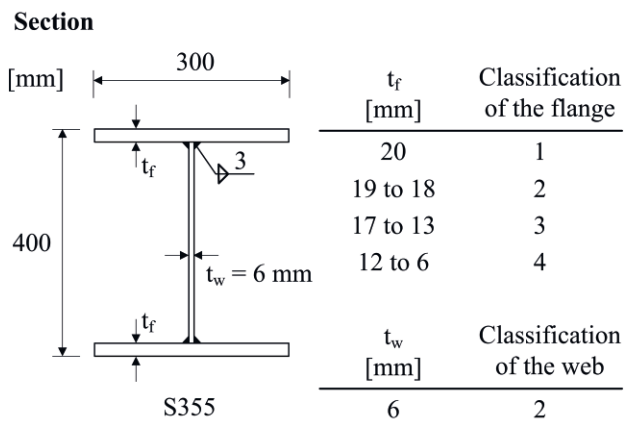
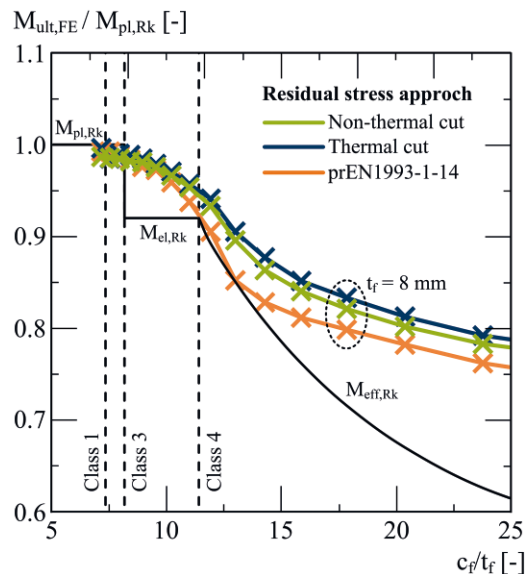


**Fig. 8** Cross-sectional load capacity in major axis bending depending on the flange slenderness

cross-section with a flange thickness of 8 mm. Fig. 9 shows the local load-displacement behaviour (left), where  $\bar{m}_i$  is the non-dimensional load factors of the major axis bending moment and  $\Delta u_z$  the vertical deflection of the local buckle as the difference between flange tip and mid flange. Fig. 9 (right) illustrates the evolution of the yield zones as a function of the non-dimensional load-factor  $\bar{m}_i$ . Here, the figure differentiates between yielding on the respective plate side to analyse the effects of local buckling.

The initial stiffness of the flange in case of local buckling is slightly lower considering the residual stress approach according to prEN 1993-1-14:2021 compared to the novel model approaches. This is mainly caused by the immediate yielding of the bottom web plate, which affects the stabilization for the flange plate. The load level for first yielding at the compression flange is related to the magnitude of the compressive residual stresses at the compression flange. Thus, this level is reached considering the residual stress approach according to prEN 1993-1-14:2021 with the lowest load-factor  $\bar{m}_i = 0.45$ , since this approach results into the highest compressive residual stresses at the flange. Here, the compression flange yields on the upper plate side of the left tip and the bottom plate side of the right tip, respectively, depending on local bending moments and subsequent local compressive stresses. Considering the approaches of the novel model, first yielding at the compression flange occurs with similar load-factors of  $\bar{m}_i = 0.60$  despite different compressive residual stresses. The higher compressive residual stresses of the novel model considering thermal cuts are composed by the beneficial location of the yield zone at the inner flange. After first yield at the compression flange, the yield zone spreads towards mid flange with decreasing stiffness, independent of the residual stress approach. Ultimate loads are reached, characterized by significantly developed yield zones in the compression flange and the compressed web.



## Local buckling

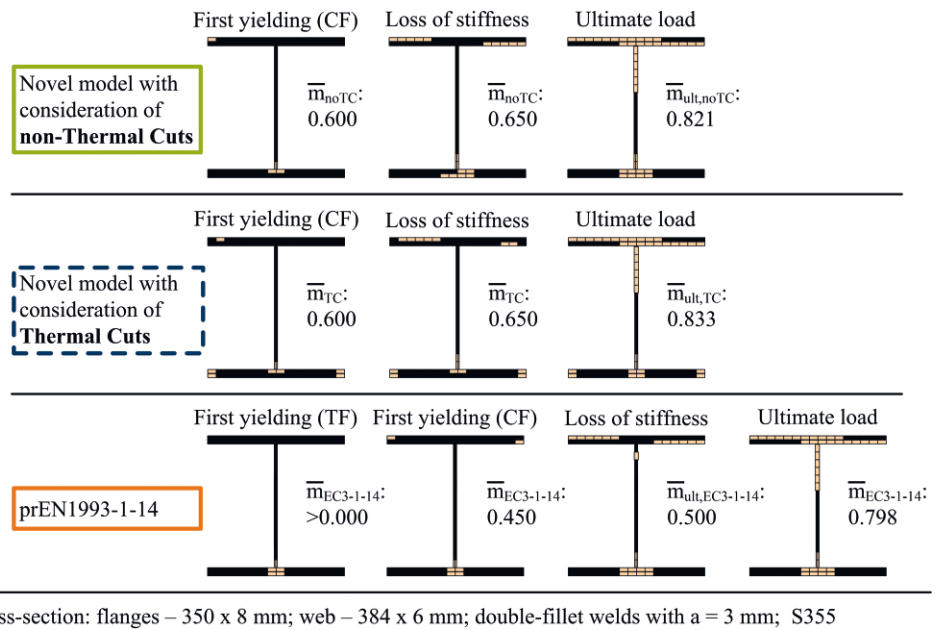
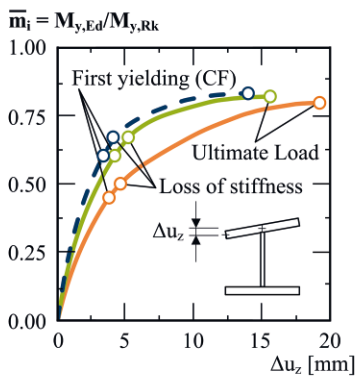


Fig. 9 Development of yield zones in case of local buckling depending of the residual stress approach

## 5 Conclusion

This article has applied a novel residual stress model for welded doubly and mono-symmetric I-sections to analyse the effect of residual stresses on the structural stability behaviour of steel members considering different cutting and welding technologies. The novel model assigns a specific residual stress distribution to each cross-section, depending on the cross-section geometry and the steel grade. In addition, the model offers the possibility of taking thermal or non-thermal cutting processes into account in fabrication of the raw steel plates. This enables a significantly better and more realistic representation of the residual stresses than with the previously used models as well as easy application in research and engineering practice.

Based on the results of the comprehensive numerical study on the impact of residual stress approaches on both the member stability behaviour and the local stability behaviour, the following conclusions are drawn:

- Thermal cutting leads to tensile residual stresses at the flange tips which result in increased compressive residual stresses at the flanges. These increased compressive residual stresses lead to lower resistances in case of major axis flexural buckling when compared to residual stress models without thermal cuts. In case of minor axis flexural buckling, lateral torsional buckling as well

as local buckling, however, similar load capacities were determined using the residual stress approaches with and without consideration of thermal cuts. For simplicity, the application of the novel model with the consideration of thermal cuts is recommended for a consistent analysis of the structural stability behaviour, which also corresponds to the normal fabrication practice.

- Both the cross-section geometry and the weld thickness affect the residual stress distribution, especially the flange compressive residual stresses. The greatest effect has been found for medium relative slendernesses and especially for major axis flexural buckling.
- The residual stress approach can significantly affect the load-carrying capacity of class 4 cross-sections with slender flanges, where it was shown that the consideration of the novel residual stress model leads to higher capacities compared to the residual stress approach according to prEN 1993-1-4:2021.
- The impact of residual stresses on the stability behaviour of high-strength steel members is less significant than for mild steel members, which can lead to improved buckling behaviour for high strength steel members. Thus, an adjustment of buckling reduction factors and a more economical design of high-strength steel structures are possible.

Open access funding enabled and organized by Project DEAL.

## References

- [1] European Convention for Constructional Steelwork (ECCS) – Technical Committee 8 (1984) *Ultimate Limit State Calculation of Sway Frames with Rigid Joints*. ECCS-Publication No. 33, Brussels, Belgium.
- [2] CEN/TC250: Eurocode 3 (2021) *Design of steel structures – Part 1-14: Design assisted by finite element analysis*. CEN/TC 250/SC3/N3296, Draft, 2.2021.
- [3] Schaper, L.; Jörg, F.; Winkler, R.; Kuhlmann, U.; Knobloch, M. (2019) *The simplified method of the equivalent compression flange – development based on LTB tests and residual stress measurements*. Steel Construction 12, No. 4, pp. 264–277. <https://doi.org/10.1002/stco.201900033>
- [4] Unsworth, D.; Driver, R.G.; Li, L.; Twizell, S.; Imanpour, A. (2021) *Characterization of residual stresses for LTB simula-*

- tions of modern welded girders. *Journal of Constructional Steel Research* 183, pp. 1–17.
- [5] Yang, B.; Zhu, Q.; Nie, S.; Elchalakani, M.; Xiong, G. (2018) *Experimental and model investigation on residual stresses in Q460GJ thick-walled I-shaped sections*. *Journal of Constructional Steel Research* 145, pp. 489–503.
- [6] Tankova, T.; Rodrigues, F.; Leitão, C.; Martins, C.; Simões da Silva, L. (2017) *Lateral-torsional buckling of high strength steel beams: experimental resistance*. *Thin-Walled Structures* 164, 107913.
- [7] Prawel, S. P.; Lee, G. C. (1974) *Bending and buckling strength of tapered structural members*. *Welding Research Supplement* 1, pp. 75–84.
- [8] Tankova, T.; Simões da Silva, L.; Balakrishnan, M.; Rodrigues, D.; Launert, B.; Pasternak, H.; Tun, T. Y. (2019) *Residual stresses in welded I section steel members*. *Engineering Structures* 197, 109398.
- [9] Käsmeier, M. (2015) *Tragverhalten und Tragfähigkeiten von stabilitätsgefährdeten Trägern und Stützen bei kombinierter Beanspruchung* [Phd. Thesis]. Ruhr-Universität Bochum.
- [10] Chacón, R.; Mirambell, E.; Real, E. (2009) *Influence of designer-assumed initial conditions on the numerical modeling of steel plate girders subjected to patch loading*. *Thin-Walled Structures* 47, pp. 391–402. <https://doi.org/10.1016/j.tws.2008.09.001>
- [11] Granath, P. (1997) *Behavior of Slender Plate Girders Subjected to Patch Loading*. *Journal of Constructional Steel Research* 42, 1, pp. 1–19.
- [12] BSK 94 (1994) *Boverkets handbok om stålkonstruktioner. (Swedish regulations for steel structures)*. Boverket, Karlskrona. In Swedish.
- [13] Schaper, L.; Tankova, T.; Simões da Silva, L.; Knobloch, M. (2022) *A novel residual stress model for welded I-sections*. *Journal of Constructional Steel Research* 188, 107017, pp.1–17. <https://doi.org/10.1016/j.jcsr.2021.107017>
- [14] Baddoo, N.; Sansom, M.; Pimentel, R.; Lawson, M.; Chen, A.; Meza, F.; Gardner, L.; Yun, X.; Zhu, Y.; Schaffrath, S.; Bartsch, H.; Eyben, F.; Simões da Silva, L.; Tankova, T.; Rodrigues, F.; Lehnert, T.; Gong, F.; Dürr, A. (2021) *Stronger Steels in the Built Environment (STROBE)*. Final report, Research Fund for Coal and Steel, GA 743504.
- [15] Knobloch, M.; Kuhlmann, U. (01.04.2017 – 01.04.2020) *Simplified Method for Lateral Torsional Buckling – Consistent Model for Welded Beams at Ambient and Elevated Temperatures*. AiF/IGF project no. 19439 N.
- [16] Dassault Systems/Simulia (2014) *Abaqus, v. 6.14*, [software]. Providence, RI, USA.
- [17] Kuhlmann, U.; Jörg, F.: *Interaction relations of normal force, bending moment and torsion: Harmonization and supplementation of verifications methods for hot-rolled steel members*. Research Report 2/2019. Düsseldorf: German Committee for Steel Construction (DASt), 2019.
- [18] CEN/TC250, FprEN1993-1-1 (2022) *Eurocode 3: Design of steel structures – Part 1-1: General rules and rules for buildings*. CEN/TC250/SC3/WG1/N3502, Draft, 11.2021

#### Authors

Dipl.-Ing. Lukas Schaper (corresponding author)  
Lukas.Schaper@rub.de  
Ruhr-Universität Bochum  
Chair of Steel, Lightweight and Composite Structure  
Universitätsstraße 150  
44801 Bochum, Germany

Trayana Tankova, PhD  
T.Tankova@tudelft.nl  
Delft University of Technology  
Faculty of Civil Engineering and Geoscience  
Department of Engineering Structures, Steel and Composite Structures  
Stevinweg 1  
2628 CN Delft, Netherlands

Prof. Luís Simões da Silva  
luisss@dec.uc.pt  
University of Coimbra  
ISISE, Department of Civil Engineering  
Rua Luís Reis Santos  
3030-788 Coimbra, Portugal

Prof. Dr. Markus Knobloch  
Markus.Knobloch@rub.de  
Ruhr-Universität Bochum  
Chair of Steel, Lightweight and Composite Structure  
Universitätsstraße 150  
44801 Bochum, Germany

#### How to Cite this Paper

Schaper, L.; Tankova, T.; Simões da Silva, L.; Knobloch, M. (2022) *Effects of state-of-the-art residual stress models on the member and local stability behaviour*. *Steel Construction* 15, No. 4, pp. 244–254. <https://doi.org/10.1002/stco.202200027>

This paper has been peer reviewed. Submitted: 29. August 2022; accepted: 18. October 2022.